APPLICATION OF LASER BASED ULTRASOUND FOR NDE OF DAMAGE IN THICK STITCHED COMPOSITES

Robert F. Anastasi
U.S. Army Vehicle Technology Center, ARL, AMSRL-VT-S
Nondestructive Evaluation Sciences Branch
NASA Langley Research Center
Hampton, VA 23681
Phone 757-864-3391

Adam D. Friedman and Mark K. Hinders
Department of Applied Sciences
The College of William and Mary
Williamsburg, VA 23187

Eric I. Madaras
Nondestructive Evaluation Sciences Branch
NASA Langley Research Center
Hampton, VA 23681

ABSTRACT

As design engineers implement new composite systems such as thick, load bearing composite structures, they must have certifiable confidence in structure's durability and worthiness. This confidence builds from understanding the structural response and failure characteristics of simple components loaded in testing machines to tests on full scale sections. Nondestructive evaluation is an important element which can provide quantitative information on the damage initiation, propagation, and final failure modes for the composite structural components. Although ultrasound is generally accepted as a test method, the use of conventional ultrasound for *in-situ* monitoring of damage during tests of large structures is not practical. The use of lasers to both generate and detect ultrasound extends the application of ultrasound to *in-situ* sensing of damage in a deformed structure remotely and in a non-contact manner. The goal of the present research is to utilize this technology to monitor damage progression during testing.

The present paper describes the application of laser based ultrasound to quantify damage in thick stitched composite structural elements to demonstrate the method. This method involves using a Q-switched laser to generate a rapid, local linear thermal strain on the surface of

the structure. This local strain causes the generation of ultrasonic waves into the material. A second laser used with a Fabry-Perot interferometer detects the surface deflections. The use of fiber optics provides for eye safety and a convenient method of delivering the laser over long distances to the specimens. The material for these structural elements is composed of several stacks of composite material assembled together by stitching through the laminate thickness that ranging from 0.5 to 0.8 inches. The specimens used for these nondestructive evaluation studies had either impact damage or skin/stiffener interlaminar failure. Although little or no visible surface damage existed, internal damage was detected by laser based ultrasound.

INTRODUCTION

Nondestructive evaluation is a standard component of aviation safety programs, where it is used to provide quantitative information on the presence and degree of damage in aviation structures. Engineers are also recognizing the value of nondestructive evaluation as a tool that could be used in laboratories during the development phases of new materials and structures. The goal is to use such laboratory testing to continuously monitor a structure's health and identify damage initiation, propagation, and final failure modes. The demands on these types of nondestructive evaluation techniques are different in a laboratory environment because of the potential for dynamic testing. This is leading to system improvements that also represent opportunities for the aviation industry.

Ultrasonics is an example of such an opportunity. Ultrasound is a well accepted test methodology used in the aviation industry, but the use of conventional ultrasound for in situ health monitoring of damage evolution during a laboratory test is not currently practical. A system improvement for ultrasonics is the use of lasers to both generate and detect ultrasound. This extends the application of ultrasound to in situ sensing of damage in a deformed structure remotely and in a non-contact manner. Using this technology in a laboratory setting will allow the testing of sub-components, components and then full scale test articles. It will also generate the knowledge base for application of this unique technology to new commercial aviation structures.

Laser ultrasonic generation and interferometric detection methods have been described in detail by other authors, (Scruby and Drain, 1990; Monchalin and Heon, 1986; Wagner, 1990; Hutchins, 1988; Monchalin et al. 1989). Ultrasound is generated by laser pulses rapidly heating a thin material surface layer. This small heated volume expands creating stresses that act as a source of elastic waves in the material. The resulting surface displacement, u, in an isotropic material, using a simple one-dimensional model is given by (Scruby and Drain, 1990),

$$u = \frac{(1+\nu)}{(1-\nu)} \frac{\alpha \delta E}{\rho C} \tag{1}$$

where ν is the Poisson's ratio, α is coefficient of linear expansion, δE is absorbed laser pulse energy assumed to have a uniform energy distribution, ρ is the material density, and C is the specific thermal capacity of the material. More recently, authors have developed analytical and numerical models that take into account thermal conductivity (Telschow and Conant, 1990) and laser beam intensity distributions in orthotropic material (Dubois et al., 1994). These more advanced models may help understand the generation of ultrasound by non-uniform laser beam intensity distributions in anisotropic composite materials. Two additional mechanisms for generating ultrasound occur when material is melted or ablated by the laser, and when that material surface is constrained by paint or other thin layer. The amplitude of the elastic waves by both these methods can be 100 times greater then those generated by thermoelastic expansion. However, the ablation process damages the material and painting may not always be possible.

Typical ultrasonic vibrations generated by normal piezoelectric or laser sources have a 1 to 50 nanometer amplitude and 100 kHz to 10 MHz frequency range. Backscatter of a probe laser beam is used to detect this ultrasonic vibration and convert it to an electronic signal. The vibrating surface causes the backscatter laser wavelength to be modulated by the vibrating surface. The Doppler effect describes how the wavelength of light reflected from the vibrating surface is shifted by an amount proportional to the surface velocity. This shifted wavelength, λ_s is given by

$$\lambda_s = \left(1 - 2\frac{\vee}{c}\right)^{-1} \lambda_0 \tag{2}$$

where $\vee$ is the velocity of the vibrating surface, c is the speed of light and λ_0 is the unshifted laser wavelength. Two interferometric methods are capable of detecting this wavelength modulation: optical heterodyning and velocity interferometry. In the first method a reference beam is made to interfere with an ultrasonic encoded beam. In the second method, the ultrasound encoded beam is made to interfere with a split portion from itself which is time delayed. The first method is limited by its low light gathering efficiency caused by backscatter from optically rough surfaces. The Fabry-Perot interferometer, a multiple wave velocity interferometer, over comes this light gathering inefficiency.

The classic Fabry-Perot interferometer is composed of two plane partially reflecting mirrors separated to form a cavity. When light from the vibrating surface enters the cavity, multiple reflection are generated between the partial mirrors with some light transmitted and reflected out of the cavity. The relation governing the intensity of light transmitted, I_t , given by (Born and Wolf, 1964) is

$$I_t = \frac{(1-R)^2}{(1-R)^2 + 4R\sin^2(\phi)} I_i \tag{3}$$

where I_i is the intensity of incident light, R is the reflectivity of the mirrors, and $\phi=(2\pi nL/\lambda_i)\cos\theta$ is the phase difference due to the mirror separation, in which n is the index of refraction of the cavity, L is cavity length or mirror separation, λ_i is the incident optical wavelength, and θ is the angle of incidence of light upon the mirror.

The connection between the Fabry-Perot interferometer and modulated backscatter can be seen in the phase term of equation (3). When ultrasonic vibrations move the surface of a structure they cause a Doppler shift in the wavelength of light backscattered from the probe laser beam. Thus, substituting the Doppler shifted wavelength λ_s, in equation (2) for λ_i in equation (3), illustrates how the Fabry-Perot interferometer signal will be modulated by the ultrasonic vibration.

SYSTEM DESCRIPTION

Figure 1, shows major components of the laser based ultrasonic system including the generation and detection lasers, Fabry-Perot interferometer, and some optical components. The complete system consists of a PC computer, 100 MHz, 8 bit analog to digital board, encoder board, translation stage controller, and translation stage with axis encoders and cable drivers. The generation and detection lasers are Nd:YAG lasers, one for ultrasonic generation and the second for detection. The generation laser is a pulsed laser with a wavelength of 1064 nm, 6.5 mm beam diameter, and a variable pulse energy up to 200 mJ with a 12 nsec pulse duration. The detection laser is a continuous wave laser with a 532 nm wavelength, 0.32 mm beam diameter and 400 mW maximum output power.

The system is operated using a PC-based virtual instrument controller and data acquisition package that stores ultrasonic A-scan signals. The main control screen has control buttons and graphics that allow the user to see scanner motion, signals, and an image of the scanned area. Ultrasonic signals are digitized to eight bit resolution at sampling rates of 6.25, 12.5, 25.0, 50.0 or 100 MHz. These are chosen by the user and can have up to 4000 points in length. The scanning area, also user selectable, can have a width of 24 inches, length of 36 inches, and can be scanned with a spatial resolution of 0.05 inches to 1.00 inch.

The system is being developed for inspecting large samples in a structural testing laboratory. The large open laboratory area raises concerns for eye safety. This system incorporates fiber optics to deliver generation and detection laser beams and to transmit the laser reflections back to the interferometer. Fiber optic cables allow the laser sources to be remote and contained. The inspection end of the fiber optic cables are attached to the scanning stage that translates the cables and thus the laser beams across the sample surface in a raster pattern. It can be enclosed to contain laser beam reflections, making the system eye safe. The system is currently being assembled and tested in an optics laboratory with three fiber optic cables to deliver and detect laser energy. Reducing the number of fibers is presently being pursued by using partial mirrors, polarizers, and filters to control laser energy delivery to and from the sample.

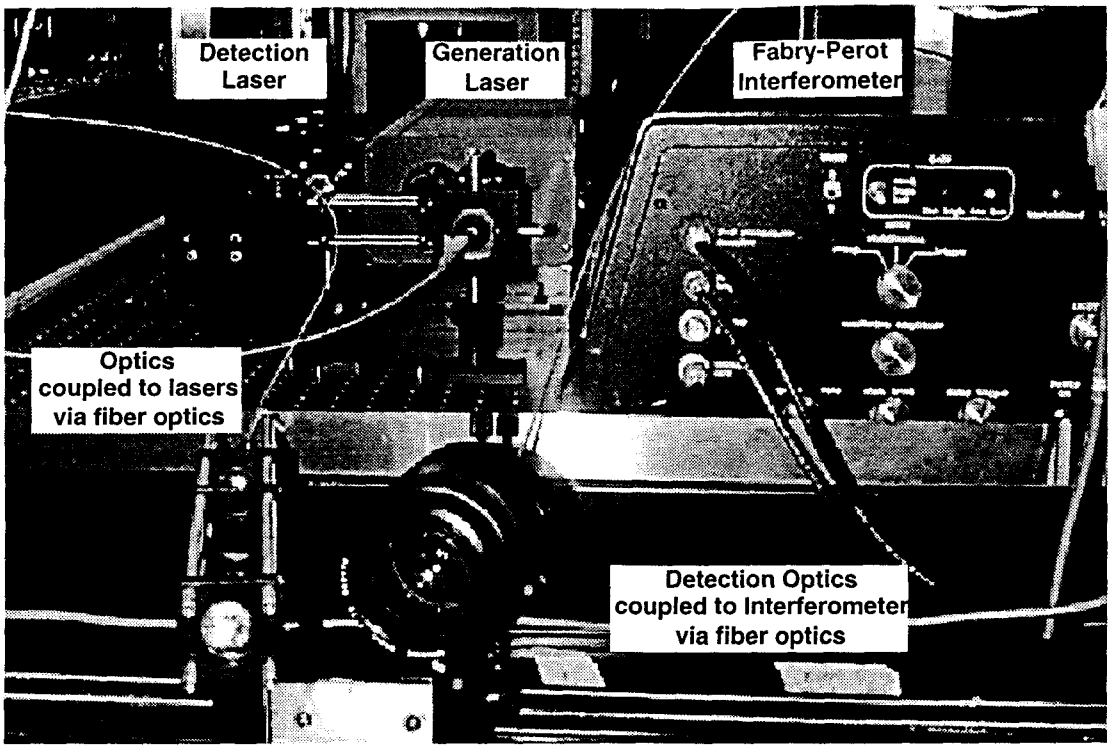

Figure 1. Laser Ultrasonic System Lasers, Fabry-Perot Interferometer, and Optics.

TEST SPECIMENS AND TESTING

Specimens evaluated in this study were obtained from a composite wing stub box that had been structurally tested to failure. The stub box is shown in Figure 2, between the extension box and a transition box. The skin consists of ten stacks of $[45/-45/0_2/90/0_2/-45/45]$ AS-4-3501-6 graphite epoxy material stitched together, resulting in a 0.58 inch total thickness. Stitched reinforcements of kevlar are in rows spaced 0.2 to 0.5 inches apart with stitch spacing approximately 0.1 inches.

A flat plate specimen was impact damaged in a drop weight test machine to create internal delaminations. A one inch diameter impact head weighing 25.25 lb. was dropped from a height of 3 ft 11.5 inches to generate an impact energy of 100 ft-lb. This produced a dent approximately 1 mm in depth and small localized cracks on the back surface of the panel. A second specimen has bi-directional T-stiffeners attached to the skin with through-the-thickness stitches. Stiffeners are made of the same material as the skin. During wing box structural testing this joint failed in regions along the intercostal/skin interface. These samples (see Figure 3) show no damage from the top surface.

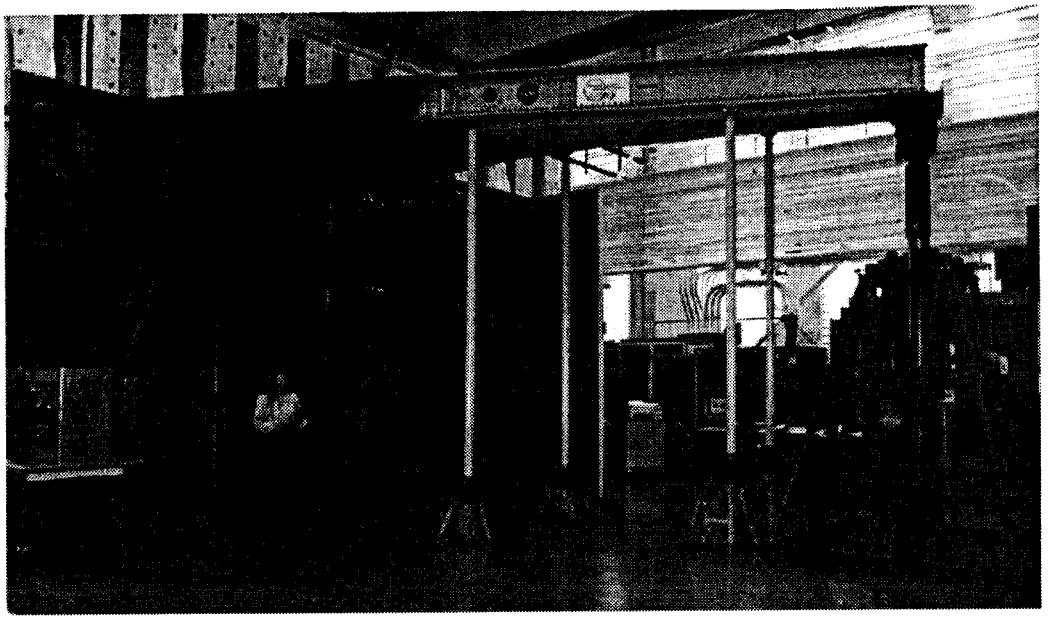

Figure 2. The Composite Wing Stub Box (above the person in photograph) is located between a metal extension box (show center to right side of the photo) and a metal transition box attached to the wall. The metal boxes were used to form realistic loads in the Wing Stub Box.

These samples were laser ultrasonically scanned in the laboratory by placing them 8-10 inches from the system optics. The generation and detection beams at the sample surface were approximately 5 mm and 2 mm in diameter, respectively. The scanned area on the impacted plate was 2.5 inches by 2.5 inches with a 0.05 inch spatial resolution. Scanning on the stiffened plate was 6.0 inches by 6.0 inches with a 0.10 inch spatial resolution. Amplitude C-scans or density plots were generated during the scanning process by gating the A-scan signal and plotting the amplitude signal under the gate as a color or gray level. A-scans were stored to file and were post-processed for evaluation. Contour plots of the same data helped highlight the contrast between stitching rows and damaged and undamaged regions.

To improve imaging of internal damage, stored A-scans were processed using methods similar to those described by (Gammell, 1981) and (Smith et al. 1989, 1991). In the first processing step, signals were time gain amplified to account for reduced echo amplification due to material attenuation. To remove some amplified noise, generated by this operation, signals were band-pass filtered in the frequency domain and then transformed back into the time domain from which the magnitude of the analytic signal was calculated. This signal processing resulted in a smooth positive value function which is an envelope of the filtered signal. Signal bandwidth was in the range of 1 to 5 MHz.

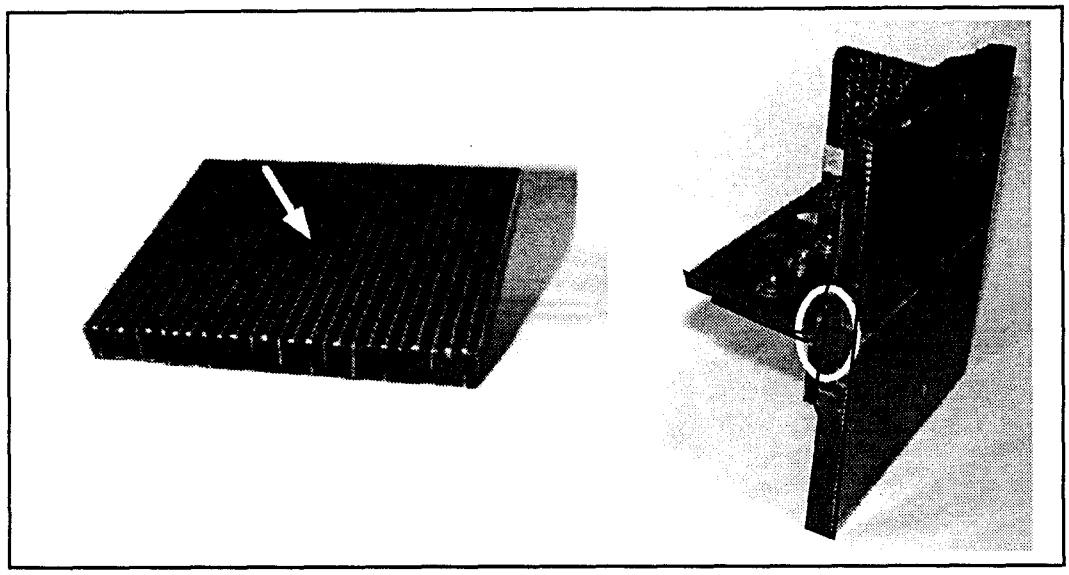

Figure 3. Thick Stitched Composite Samples, (left) Impacted Plate with dimensions 4.5" x 5.5" x 0.58" and (right) Bi-directional Skin/Stiffened Plate with interlaminar failure (circled in photograph) with dimensions 7.0" x 7.0" x 0.58".

RESULTS AND DISCUSSION

Through-the-thickness stitches in composites produce several effects on ultrasonic imaging. One is caused by increased interlaminar shear strength which moderates the damage and subsequent image. In conventional composites, impact damage image would present itself as an irregular shape about the impact site, preferentially oriented along ply directions in the lamina. In stitched composites, the impact site tends to be circular because through-the-thickness stitches increase interlaminar shear strength which slows and contains delamination progression. Secondly, these through the thickness stitches also perturb ultrasound transmission (Long, et al 1990) because the sound velocity is greater in the stitching than the surrounding material. These perturbations cause a phase-distorted wavefront at the material surface or point of ultrasonic detection and produce a reduced signal amplitude. Both these effects are visible in Figure 4, as a dark circular area and light and dark bands. This figure was generated by measuring the amplitude of the back surface ultrasonic echo. Spacing between the bands is approximately 0.2 inches and corresponds to stitch spacing in the sample. Representative A-scan signals from these areas are shown in Figure 5. A conventional ultrasonic signal with a back surface echo is shown in Figure 5a, which represents a signal from light band regions. The back wall echo occurs approximately 10 microseconds after the front wall signal. A representative signal from the dark band region, shown in Figure 5b, lacks a back surface echo and has reduced interior echoes. A signal from the dark circular area, shown in Figure 5c, also lacks a back surface echo but has large echoes

occurring during the first five microseconds from internal damage near the front surface. This circular region is approximately 2.25 inches in diameter and results from the one inch diameter impactor that created only a millimeter depth indentation on the sample surface. A third interesting feature in Figure 4 is seen at the center of the damage, where there is evidence that sound penetrates to the back wall at certain points in spite of the damage. The stitches may be partially responsible for the transmission of ultrasound within this area of impact. If the through-the-thickness stitches do not break during the impact, it is possible that they act as waveguides for the sound to travel to the back wall and back. While in other location in the damage area, sound travel to the back wall is blocked. Therefore, at these locations no phase cancellation occurs and some waveguided signals are detected. For comparison to the laser based ultrasonic scan of Figure 4, a water-tank C-scan was performed on the same impact sample and is shown in Figure 6. This water-tank, peak detected scan, was generated using a 5 MHz, 0.5 inch diameter transducer. Stitching and damage as mentioned above are clearly visible and comparable to the laser ultrasonic scan. However, The water-tank scan is smoother in appearance, possibly due to a coarser resolution of the transducer compared to that of the one tenth inch diameter laser detection beam. This may also explain why the laser scan shows some signal detection in the center of the damage area while the water-tank scan does not.

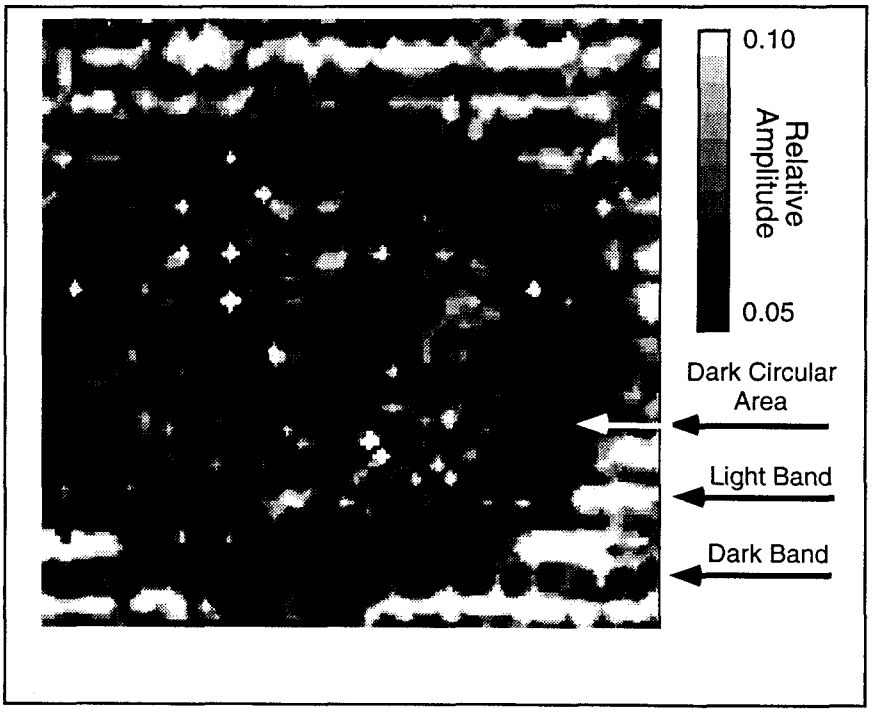

Figure 4. Peak detected back wall C-scan contour plot of impact damaged plate. Scan area is 2.5" by 2.5" and the scan spatial resolution is 0.05". The dark circular area is approximately 2.25" in diameter and horizontal lines correspond to stitching rows.

The second stitched composite sample, studied using laser based ultrasound has a complex structure consisting of a horizontal and a vertical stiffener. It is shown in Figure 3 and its horizontal and vertical profiles of varying thickness are shown along with scan results in Figure 7, Figure 8 and Figure 9. To highlight this structure ultrasonically, a back surface echo from a particular thickness was isolated and measured. Two resulting scans are shown in Figure 7. The first figure, Figure 7a, measures the echo from the skin or thinnest section of the sample. This scan shows dark horizontal and vertical lines that correspond directly to stitched rows as well as a wide dark vertical band, greater than three inches thick, that corresponds to the thicker stiffener section. This region is dark because its back surface echo is much later due to a thickness increase and is therefore ignored in the figure. The result of shifting the sampling point to detect the thicker material section is shown in Figure 7b. Here a dark horizontal and vertical band can be seen with the vertical band being about 0.7 inches thick at its widest point. These bands correspond to the horizontal and vertical webs of the stiffener, the thickness of the vertical web is approximately 0.6 inches. With a finer scanning spatial resolution these thickness values would be approximately equal. The vertical white bands represent the back wall of the thicker web and also show evidence of stitching. Taken together these show underlying structure of the sample but no substantial evidence of damage. A laser ultrasonic and water-tank peak detected scans of the stiffened sample are compared in Figure 8. The laser ultrasonic scan, Figure 8a, was generated by combining the echoes from the skin back surface and the "T" back surface for direct comparison to the water-tank scan where peak detected signals were from a glass plate beneath the sample. The water-tank scan, Figure 8b, was generated with a 5 MHz, 0.5 inch diameter

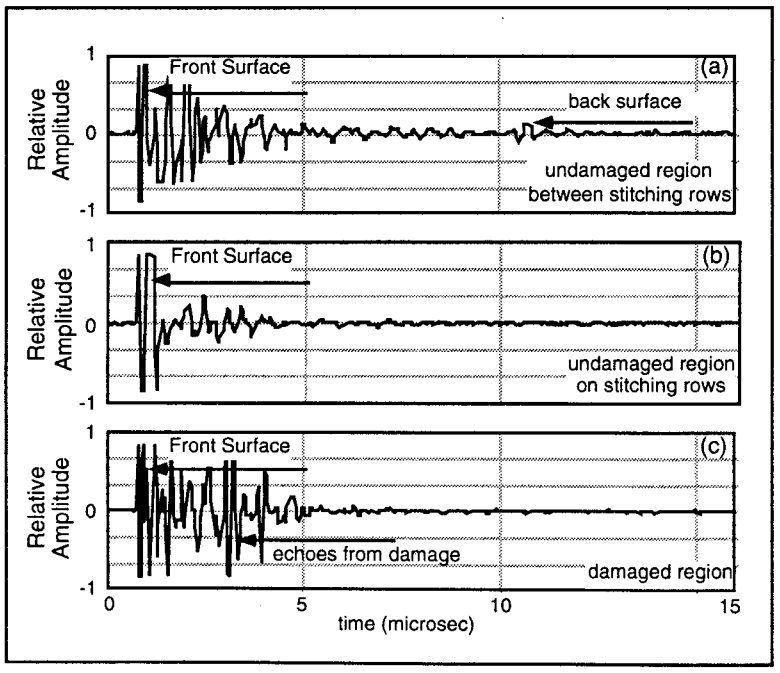

Figure 5. Representative A-scan signals from damaged and undamaged regions of impacted plate (a) form light band, (b) from dark band, and (c) from dark circular area.

transducer and scan area was 7.0 inches by 7.0 inches, slightly larger than the laser ultrasonic scan. These scans in Figure 8, both show the horizontal and vertical stitching as well as the vertical web stiffener. However, the horizontal web stiffener is not well defined, as in the laser scan of Figure 7b, possibly due to signal interference with horizontal stitches. As in the previous peak detected scans of this stiffened sample, underlying structure can be identified but substantial evidence of damage can not.

To highlight internal damage, a third image was created by plotting the location in time of the back wall echo instead of the amplitude. Damage would be highlighted if the echo occurred earlier than anticipated. The result in Figure 7, shows evidence of damage located above the horizontal stiffener region, on the left and right sides. The circled region on the scan corresponds to the left side of the sample and is circled and outlined in the picture. This delamination occurs about the same depth as the thinnest back wall section. Thus the time-of-flight to the delamination is similar to the time-of-flight to the back wall of the skin, seen in the four corners of the scan. If the sample was undamaged, these regions would be shaded gray instead of black. In an intact wing structure, this stiffener flaw would be internal to the structure and could be over looked if visual examination of back and side surfaces were not possible.

These scans demonstrate that laser generated and detected ultrasound via fiber optic cable is capable of detecting damage in thick stitched composite material in situ. Fiber optic cable provides a means of delivering eye hazardous laser energy to the inspection area in order to generate and detect ultrasound in a non-contact manner to monitor structural health and ultrasonically map internal damage and underlying structure.

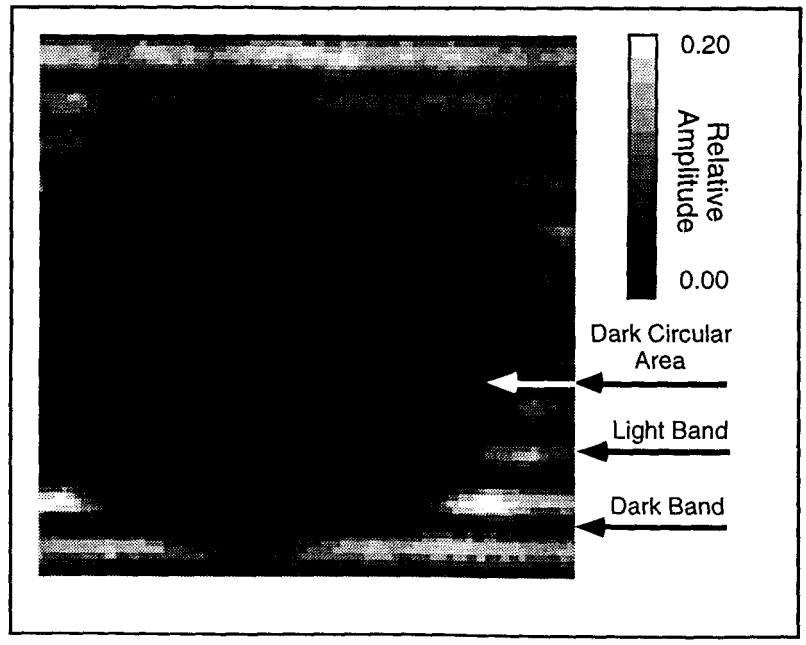

Figure 6. Water tank C-scan of impacted plate for comparison to Laser Based Ultrasound C-scan shown in Figure 4.

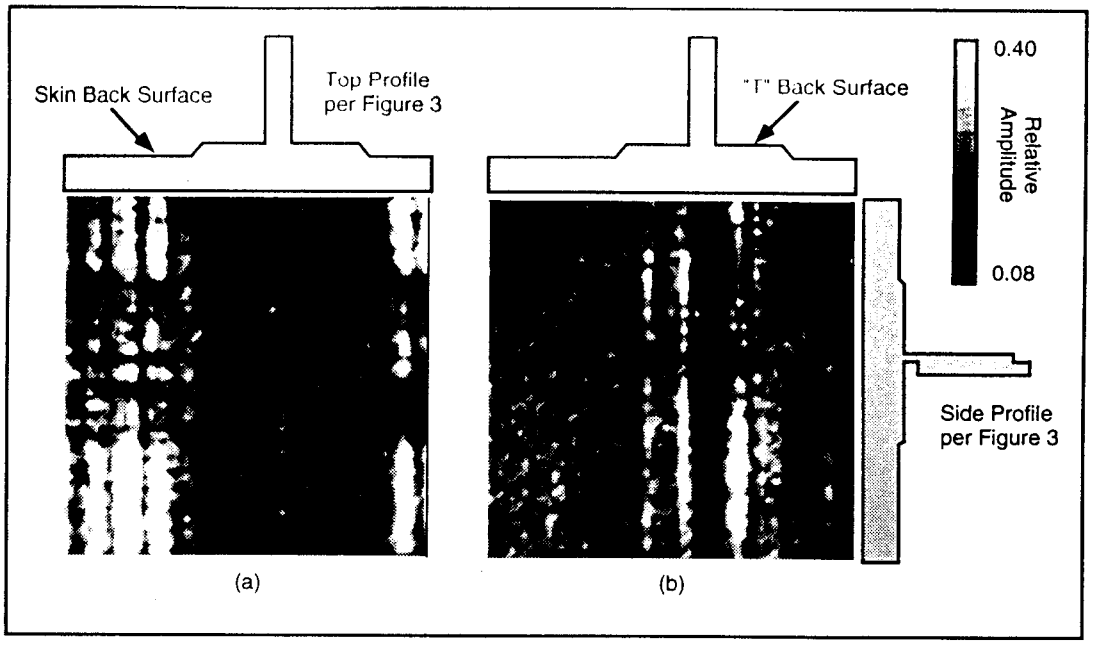

Figure 7. Peak detected back wall C-scan contour plots of bi-directional skin/stiffened sample with; (a) gate over skin back surface and (b) gate over thicker "T" back surface.

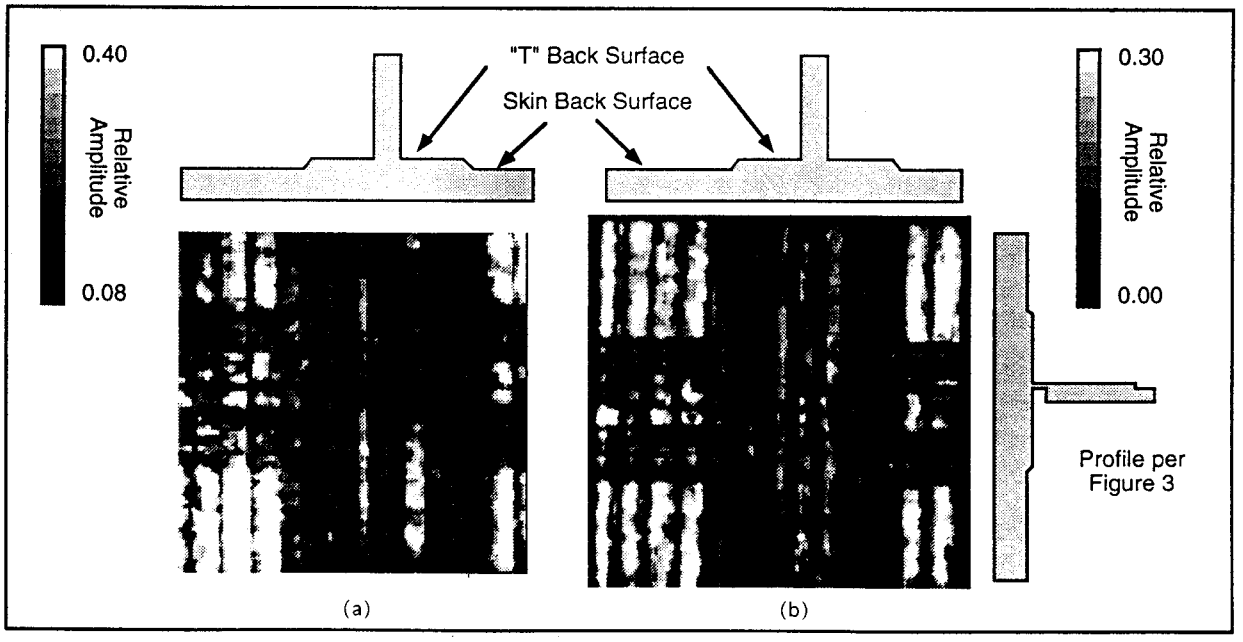

Figure 8. Peak detected C-scan comparison, (a) laser ultrasonic scan and (b) water-tank scan.

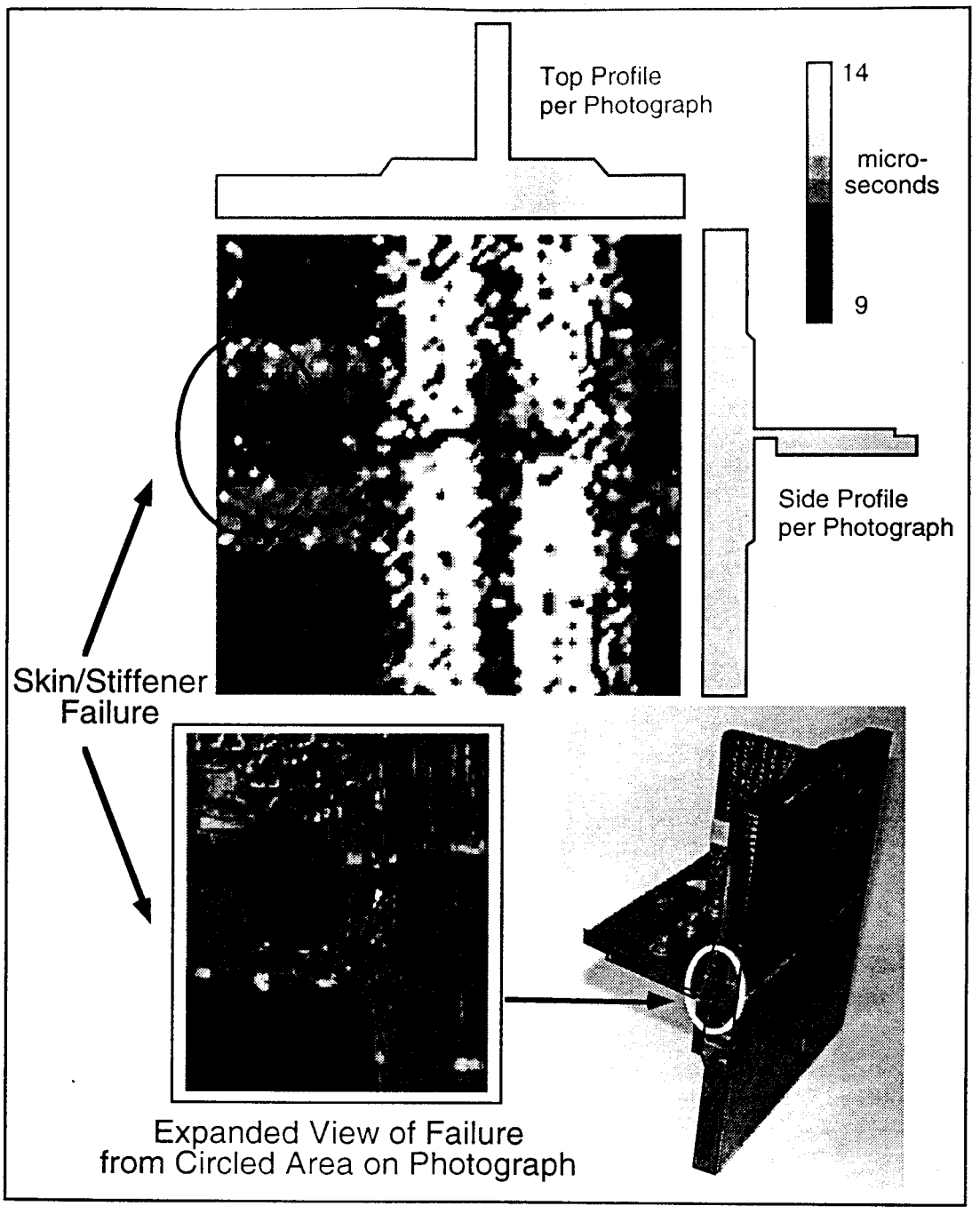

Figure 9. Time-of-Flight C-scan contour plot of bi-directional skin/stiffened sample showing skin/stiffener failure areas.

REFERENCES

Born, M. and E.Wolf, *Principles of Optics*, Pergamon Press, New York, 1964.

Dubois, M., F. Enguehard, M. Choque, J.-P. Monchalin, and L. Bertrand, "Numerical Modeling of Laser Generation of Ultrasound in Orthotropic Materials," in *Review of Progress in Quantitative Nondestructive Evaluation*, Vol. 13, Edited by D.O. Thompson and D.E. Chimenti, Plenum Press, New York, 1994.

Gammell, P.M., "Improved Ultrasonic Detection using the Analytic Signal Magnitude," *Ultrasonics*, Vol. 19, March 1981.

Hutchins, D.A., *Ultrasonic Generation by Pulsed Lasers*, Physical Acoustics. Vol. 18, 1988.

Long, E.R., S.M. Kullerd, P.H. Johnston, and E.M. Madaras, "Ultrasonic Detection and Identification of Fabrication Defects in Composites," Presented at the First NASA Advanced Composite Technology Conference, Seattle, Washington, NASA Technical Report #CP3104, October 29 - November 1, 1990.

Monchalin, J.-P., "Optical Detection of Ultrasound," *IEEE Transactions on Ultrasonics, Ferroelectrics, and Frequency Control*, Vol. UFFC-33, No. 5, September 1986.

Monchalin, J.-P. and R. Heon, "Laser Ultrasonic Generation and Optical Detection with a Confocal Fabry-Perot Interferometer," *Materials Evaluation*, Vol. 44, September 1986.

Monchalin, J.-P., R. Heon, P. Bouchard, and C. Padioleau, "Broadband Optical Detection of Ultrasound by Optical Sideband Stripping with a Confocal Fabry-Perot," *Applied Physics Letters*, 55(16), October 1989.

Scruby, C.B., L.E. Drain., *Laser Ultrasonics: Techniques and Applications*, Adam Hilger, New York, 1990.

Smith, B.T., J.S. Heyman, A.M. Buoncristiani, E.D. Blodgett, J.G. Miller, and S.M. Freeman, "Correlation of the Deply Technique with Ultrasonic Imaging of Impacted Damage in Graphite-Epoxy Composites," *Materials Evaluation*, Vol. 47, No. 12, December 1989.

Smith, B.T., G.L. Farley, J. Maiden, D. Coogan, J.G. Moore, "Damage Assessment and residual Compression Strength of Thick Composite Plates with Through-The-Thickness Reinforcements," in *Review of Progress in Quantitative Nondestructive Evaluation*, Vol. 10B, Edited by D.O. Thompson and D.E. Chimenti, Plenum Press, New York, 1991.

Telschow, K.L. and R.J. Conant, "Optical and Thermal Parameters Effect on Laser-Generated Ultrasound," *J. Acoust. Soc. Am.*, 88(3), September 1990.

Wagner, J.W., *Optical Detection of Ultrasound*, Physical Acoustics, Vol. XIX, Academic Press, 1990.